Article

Fibrillar organization in tendons: A pattern revealed by percolation characteristics of the respective geometric network

Daniel Andrés Dos Santos[1], **María Laura Ponssa**[2], **María José Tulli**[2], **Virginia Abdala**[1,2,3]

[1]Instituto de Biodiversidad Neotropical, Facultad de Ciencias Naturales e Instituto Miguel Lillo, Universidad Nacional de Tucumán – CONICET. Horco Molle S/N, Yerba Buena, Tucumán, Argentina

[2]Instituto de Herpetología, Fundación Miguel Lillo-CONICET. Miguel Lillo 251, San Miguel de Tucumán, Tucumán, Argentina

[3]Cátedra de Biología General, Facultad de Ciencias Naturales e IML, Universidad Nacional de Tucumán. Miguel Lillo 251, San Miguel de Tucumán, Tucumán, Argentina

E-mail: dadossantos@csnat.unt.edu.ar

Received 7 January 2014; *Accepted 10 February 2014*; *Published online 1 June 2014*

Abstract

Since the tendon is composed by collagen fibrils of various sizes connected between them through molecular cross-links, it sounds logical to model it via a heterogeneous network of fibrils. Using cross sectional images, that network is operatively inferred from the respective Gabriel graph of the fibril mass centers. We focus on network percolation characteristics under an ordered activation of fibrils (progressive recruitment going from the smallest to the largest fibril). Analyses of percolation were carried out on a repository of images of digital flexor tendons obtained from samples of lizards and frogs. Observed percolation thresholds were compared against values derived from hypothetical scenarios of random activation of nodes. Strikingly, we found a significant delay for the occurrence of percolation in actual data. We interpret this finding as the consequence of some non-random packing of fibrillar units into a size-constrained geometric pattern. We erect an ideal geometric model of balanced interspersion of polymorphic units that accounts for the delayed percolating instance. We also address the circumstance of being percolation curves mirrored by the empirical curves of stress-strain obtained from the same studied tendons. By virtue of this isomorphism, we hypothesize that the inflection points of both curves are different quantitative manifestations of a common transitional process during mechanical load transference.

Keywords percolation; collagen; fibril network; interspersion; pattern recognition.

Network Biology
ISSN 2220-8879
URL: http://www.iaees.org/publications/journals/nb/online-version.asp
RSS: http://www.iaees.org/publications/journals/nb/rss.xml
E-mail: networkbiology@iaees.org
Editor-in-Chief: WenJun Zhang
Publisher: International Academy of Ecology and Environmental Sciences

1 Introduction

It has been often stressed that collagen fibrils in a connective tissue exhibit a network organization (Purslow et al., 1998; Berthod et al., 2001; Chandran and Barocas, 2006; Rigozzi et al., 2011; Shirazi et al., 2011). It is

basically proposed that the microstructural properties of the collagen network contribute to continuum mechanical tissue properties that are strongly anisotropic with tensile-compressive asymmetry (Shirazi et al., 2011). Besides, extensible connective tissues (e.g. skin, blood vessels, fascia) contain networks of fibrillar collagen embedded into an amorphous matrix. It is the reorientation of the collagen fibres within these networks that allows large extensions of the tissues and is responsible for their non-linear stress–strain curves (Wainwright et al., 1976; Purslow et al., 1998). This characterization of the collagen organization as a network is used to explain mechanical properties of soft biological tissues. Despite distinct mechanical functions, biological soft tissues have a common microstructure in which a ground matrix is reinforced by a collagen fibril network (Purslow et al., 1998). Likewise, the existence of a collagen network in hard biological tissues such as cartilage (Långsjö et al., 2009; Långsjö et al., 2010; Julkunen et al., 2010) is also widely accepted. Collagen fibrils are not isolated functional entities, but they integrate a network system in which the proximate fibrils could exhibit a functional connection. In spite of the currently assumption that the collagen fibril network is responsible of the main mechanical properties of tendon, to our best knowledge the underlying geometrical network has been never formalized in graph terms where the nodes and edges represent the fibrils and their cross-links respectively.

The properties of connective tissues are known to depend on a wide variety of factors such as the type and maturity of the tissue, the chemical nature of the covalent cross-links, the type and quantity of the glycosaminoglycans throughout the extracellular matrix (ECM) and the content of elastic fibres, water and minerals (Parry et al., 1978).Two main classes of extracellular macromolecules make up the tendon matrix: proteoglycans (PGs), which play a complex role in force transmission and maintenance of tendon tissue structure (Reed and Iozzo, 2002; Rigozzi et al., 2010) and collagen fibrils. Studies that have investigated the relationship between structural and mechanical properties have generally focused on one major component, either collagen or proteoglycans (PG), with studies focusing on collagen fibril morphology being more common (Rigozzi et al., 2010).The amount of interactions between the collagen fibrils and the surrounding matrix influents the stiffness of the tissue, and this may prevent changes in shape after the removal of stress (Parry et al., 1978). The degree of interaction between the collagen fibrils and the amorphous matrix is function of the collagen fibril diameter distribution. The relevant role of the ECM is also visible during tendon development, because collagen fibrillogenesis generates a tendon-specific extracellular matrix that determines the functional properties of the tissue (Zhang, 2005; Zhang et al., 2005). Other studies indicate that biochemical deficiencies the amorphous ECM may be a primary causative factor in certain tendon pathologies (Battaglia et al., 2003; Mikic et al., 2001).

Networks are a collection of elements (nodes or vertices) connected by some relationships of interest (links or edges) (Zhang, 2012a, 2012b, 2012c). The internet, airline routes, and electric power grids are all examples of networks whose function relies crucially on the pattern of interconnection between the components of the system. Thinking of systems as networks and studying their patterns of connection can often lead to new and useful insights (Newman, 2010; Ferrarini, 2013, 2014; Zhang, 2012a, 2012b, 2012c, 2013). An important property of such connection patterns is their robustness—or lack thereof— to removal of network nodes, which can be modeled as a percolation process on a graph representing the network (Callaway et al., 2000). Percolation theory is a branch of probability theory dealing with properties of random media (Berkowitz and Ewing, 1998; Zhang, 2012a, 2013). It is one of the simplest models in probability theory which exhibits what is known as critical phenomenon. This usually means that there is a natural parameter in the model at which the behavior of the system drastically changes (Grimmett, 1999). Percolation statement is simple: every site on a specified lattice is independently either occupied (recruited), with probability q, or not with probability $1 - q$. In particular, the system percolates when it exhibits a continuous phase transition at a

finite value of *q* which, on a regular lattice, is characterized by the formation of a cluster large enough to span the entire system across its dimensions in the limit of infinite system size (Newman and Ziff, 2001). From a mathematical perspective, the percolation theory describes the behavior of connected clusters in a random graph (Cuestas et al., 2011). The percolation method allows us to evaluate the network resilience to deletion of network nodes (Callaway et al., 2000).

In this work we delineate a network approach for studying the tendon organization (system composed of interconnected fibrils) that could contribute to a better understanding of its biomechanical responses. Relative neighborhood networks between collagen fibrils are here erected as proxies for the underlying collagen network. This type of objects constitutes an appropriate candidate to make mathematically tractable the collagen network. The links (edges) between the discrete units (nodes) of this network are derived from the relationships of spatial proximity between fibrils. However, the spatial gap between fibrils connected by proximity is occupied by the amorphous matrix and should be also considered a relevant component for the functionality of the entire system. Amorphous matrix is assumed to be the physical substrate over which the information can flow across the nodes of the network. In dealing with the term transference of information, we adopt the meaning implicit to the information theory (Shannon, 1948) that involves the transmission of data or any state change in a system. This notion liberates us from considering the ECM network as a theoretical model uniquely associated to the context of force transmission. The model of ECM network is useful to address the topic of functional integrity. One way to do that is to evaluate if information can propagate throughout the structure of the network, or equivalently to study its characteristics of percolation. Percolation theory may contribute to the understanding of the information flow such as force transmission from the beginning of the tensile activity (tendon activated by a contractile force) until the resulting response (movement of skeletal pieces).

This paper is interested on the morphology and spatial organization of the tendon collagen fibrils in addition to their functional consequences. It is structured around the following assumptions: i) collagen fibrils are units that mediate the transmission of information; ii) the tendon is an assembly of interconnected fibrils that can be modeled with the approach of geometric networks; iii) molecular cross-links provides the material evidence about the connection between fibrils; iv) percolation of information throughout the network is directly associated to the notion of functional integrity; v) phase transition involved by the percolation threshold can be traced to a point on the non-linear stress-strain curve. In tight correspondence with the above premises, and considering a hypothetical scenario of fibril recruitment by increasing size, we ask the following questions: 1) which is the critical threshold that allows the information to traverse the physical dimensions of the network in which fibrils reside? Based on the observed percolation, 2) is it possible to infer some peculiar geometrical feature of the network structure? To answer this, we need to compare the observed percolation pattern against the random expectations under a stochastic shuffling of the fibril sizes but maintaining the topology of the network. Taking into account that percolation of a system implies a phase transition, 3) which is the influence of this putative phenomenon in the mechanical properties exhibited by tendons? Can the stress-strain curves be used to deal with the last issue? We think that a right comprehension of all these inquiries will bring us new insights to grasp the outstanding mechanical properties of the tendon.

2 Material and Methods

Electron microscopy analysis was conducted with samples of the flexor tendon of the Digit IV obtained from adults of anurans (*Scinax nasicus*, *Phyllomedusa sauvagii*, *Rhinella arenarum*, *Leptodactylus latinasus* and *Leptodactylus chaquensis*) and squamatan reptiles (*Liolaemus elongates*, *L. coeruleus*, *L. bibroni* and *Tupinambis rufescens*). Details about examined specimens are provided in the Appendix. We selected the

flexor tendon of Digit IV because of the importance of this digit in locomotion as stressed by Teixeira-Filho et al. (2001) and Tulli et al. (2011).

Samples were placed overnight in 0.1-M phosphate buffer with 2.5% glutaraldehyde and 4% paraformaldehyde. The tissue was then fixed in 1% osmium tetroxide, dehydrated in graded acetones, and flat embedded in Epon plastic 812 (Ernest F Fullam, Inc, Latham, NY) in a cross-sectional orientation. Sections (85 nm) were obtained and stained with 0.25% lead citrate and 5% uranyl acetate in 50% acetone and then observed and photographed in a JEOL100CX transmission electron microscope (LAMENOA, Universidad Nacional de Tucumán, Argentina). Collagen fibril diameters of each species were measured on each micro-graph using the Image J 1.44p (Wayne Rasband, National Institutes of Health, USA,http://rsbweb.nih.gov/ij/). Diameter of each fibril present in the selected area was measured. Each fibril included in the selected area was identified in a coordinate system using the particle analysis option of the Image J software.

2.1 The collagen fibril network

Each cross section of a tendon can be represented as a set of points distributed in a 2-dimensional space. Since these points are assumed to interchange information they give rise to a spatial network. In fact, glycosaminglycancross-links connect each fibril with the adjacent ones. To address the problem of the geometrical organization of the network, we need to operationalize the concept of the fibrillar network. Because spatial networks subsume into the category of geometric graphs, we choose this mathematical model to work with. A geometric graph $G = (V, E)$ is an embedding of the set V of nodes as points in the plane, and the set E of edges as straight line segments joining pairs of points in V. Locations for the center mass of each fibril are adopted as point occurrences of fibrils throughout the study system (here, the cross section of the tendon). We also say that the graph G is planar if no two of its edges intersect except perhaps at their end points. In the computational geometry literature, there are several classes of planar geometric graphs arising from what are known as proximity graphs (see the survey of Jaromczyk and Toussaint 1992 for more details).

In this paper, we will model the topology of the collagen fibril network via a Gabriel graph. The rationale for this choice relies on the capacity of the Gabriel graph to capture a fair representation of the proximity structure portrayed by the data. A geometric graph $G= (V, E)$ is called a Gabriel graph if the following condition holds: for any $u, v \epsilon V$, an edge $(u, v) \epsilon E$ if and only if the circle with uvas diameter does not contain any other point of V (Gabriel and Sokal, 1969) (Fig. 1). The ultimate meaning of observing two adjacent fibrils A and B in the underlying Gabriel graph (connected by an edge) is that their area of reciprocal influence is unique and not interfered by nearby fibrils. If the stress force does flow throughout the interfibrillar matrix, it would freely flow across the space bridging fibrils directly linked in the respective Gabriel graph.

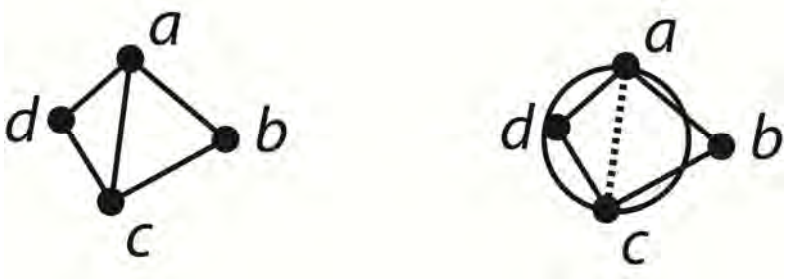

Fig. 1 Example of Gabriel graph (right) obtained from the Delaunay triangulation (left) applied on a set of 4 points, i.e. {*a*, *b*, *c* and *d*}. The edge joining *a* to*c* is discarded because it corresponds to the diameter of a circle that includes another point of the set (i.e. point *d*).

2.2 Percolation

The network of collagen fibrils is used to represent the propagation of information across the tendon. Here, information can be understood as the propagation of the mechanical stress across the tendon, or the flow of the cross-linking molecules through the amorphous matrix, or any other factor that can change the integral response of the tendon. Vertices on the graph are considered occupied or not, depending on whether the network nodes they represent (fibrils) are activated or recruited. We have examined the site percolation of the network in which the occupation is a function of the fibril size. So, we have considered percolation under a targeted activation of nodes. In this way, we have simulated a sequential recruitment of fibrils increasingly ordered by their sizes and checked then the spanning area of the putative percolating cluster.

In site percolation of spatial networks one views the clusters formed by the occupied vertices. A cluster is defined as set of neighboring or adjacent vertices that are occupied. Of particular interest is to establish if there exists a cluster that connects the borders of the area spanned by the network (here, the cross section of the tendon). Such a cluster is called a percolating cluster and its presence represents a qualitative change in the structure of the system from a disconnected state to a connected one (functionality transition). We estimate the percolation threshold (q) from the inflection point of the S-shaped curved relating the relative size of the spanning cluster and the fraction of activated sites. The following fitting model was used (Pawłowska and Sikorski, 2013):

$$P(\varphi) = 1 - \left(1 + \exp\left(\frac{\varphi - q}{a}\right)\right)^{-1}$$

where a is a parameter that dictates the slope of the curve. Here, percolation probability P is function of the fraction φ of activated sites. In operative terms, nonlinear least square regression was applied on the values of relative size of the percolating cluster against the respective fraction of activated sites. The relative size of the percolating cluster was taken as the ratio between the area of the bounding box enclosing the points of the largest component and the overall rectangular area of the system under study. Percolation threshold was calculated for the case of targeted sequential activation of nodes ordered by increasing size. In a next instance of analysis, this observed score for q was compared against values obtained from random scenarios of node activation. Certainly, if the observed value would deviates from random expectations then we could suspect some pattern of spatial organization where the size of fibrils has a prominent role.

We conducted separate recruitment scenarios for each empirical case of study. Each scenario consisted of 21 instances in a gradual sequence of node activation, using for that purpose a vector of cutoff values that dictate the activation (or not) of the nodes. Whenever a node has a size (= fibril diameter) lower or equal than a specified cutoff value it is activated. The 21 elements of the referred vector are increasingly ordered and correspond to the percentiles by steps of five (0, 5, 10, …, 100) found on the statistical distribution of fibril sizes. Thus, the first element of this vector corresponds to the minimum size of fibril, its second element corresponds to the fifth percentile, its third element is the tenth percentile, and so on. The last element concerns to the largest fibril. Although exploring the entire set of unique values of size would have yielded more accurate results, we have binned the data by percentile intervals of five because of computational facilities. The full activation of nodes translates into the original Gabriel graph that accounts for the collagen fibril network. As the activation of nodes proceeds from the minimum cutoff value to the maximum one, nodes are connected by an edge if they are actually neighbors in the underlying Gabriel graph. The critical instance, or scene, of the recruitment scenario is that where the percolating cluster firstly appears. The inflection point on the percolation curve, obtained by adjustment of the above equation to the 21 instances of node activation, was used to estimate the percolation threshold q. The q quantile for the set of fibril diameters was subsequently

employed for inferring the critical size for fibril activation around which percolation occurs.

To test the significance of the observed values of percolation, we compared them with scores obtained via random simulations. We conserved the network topology and changed the original assignment of size values among the nodes. We set the level of significance at 5% over a total of 100 random simulations. Rejection of null hypothesis would suggest a geometrical pattern shaped by the size of the collagen fibrils.

2.3 Balanced interspersion of heteromorphic fibrils

We will consider a model of non-random interspersion to explain the particular arrangement of polymorphic fibrils, i.e. a pattern where a given fibril is surrounded by others of dissimilar size. We will study an algorithmic arrangement of fibrils on a square lattice able to mimic the percolating behavior observed across the empirical cases of study.

2.4 Stress-strain relationship and inflection point

Tendon samples of *Leptodactylus chaquensis*, *Phyllomedusa sauvagii*, *Rhinella arenarum* and *Tupinambis rufescens* were carefully aligned and gripped using Instron® at room temperature located at Facultad de Odontología, Universidad Nacional de Tucumán. Tendons were tested in tension up to break at the same elongation rate of 0.033 mm/s. Initial gauge length and width of specimens were measured before performing the tensile test. Once the ultimate tensile strength was achieved, we decided to report any additional reading of stress-strain above the 90% of this maximum caused by the gradual breakage of tendons by defibrilation.

Curves were generated through piecewise-cubic splines on the raw data. The inflection point of a curve is the geometrical place where a change of concavity is produced, and they are linked with phase transitions in the dynamics of a system. We estimated the inflection point directly from the raw data following the methodology of Christopoulos (2012). In the context of this paper, the inflection point corresponds to the transition from a convex strain-stress response to a concave one. All statistical and network analyses were performed with the R platform (R Core Team, 2012). The scripts are available from heading author upon request. This study was approved by the Ethics Committee of Universidad Nacional de Tucumán.

3 Results

The Fig. 2 shows the distributions of the fibrils according to their size. The box plots show a segregation of the data in three pools clearly distinguishable: one composed by small fibrils (the majority less than 50 nm), another conformed by medium fibrils (most of them between 50 and 100 nm), and other by large fibrils (the majority of them larger 100 nm). Segregation of the taxa proceeds regardless of the phylogeny. The range of variability of fibril size seems to increase in direct relationship with the median of fibrils.

3.1 Percolation

The Fig. 3 shows two scenes taken from the progressive recruitment process, namely (i) the scene concerning to the stage near to the formation of the percolating cluster, (ii) the scene concerning to the stage immediately posterior to the formation of the percolating cluster. The percolation corresponds to the inflection point in the fitted S-shaped curves relating quantile probabilities and fraction of spanning area. Percolation thresholds calculated for the empirical cases are in Table 1.

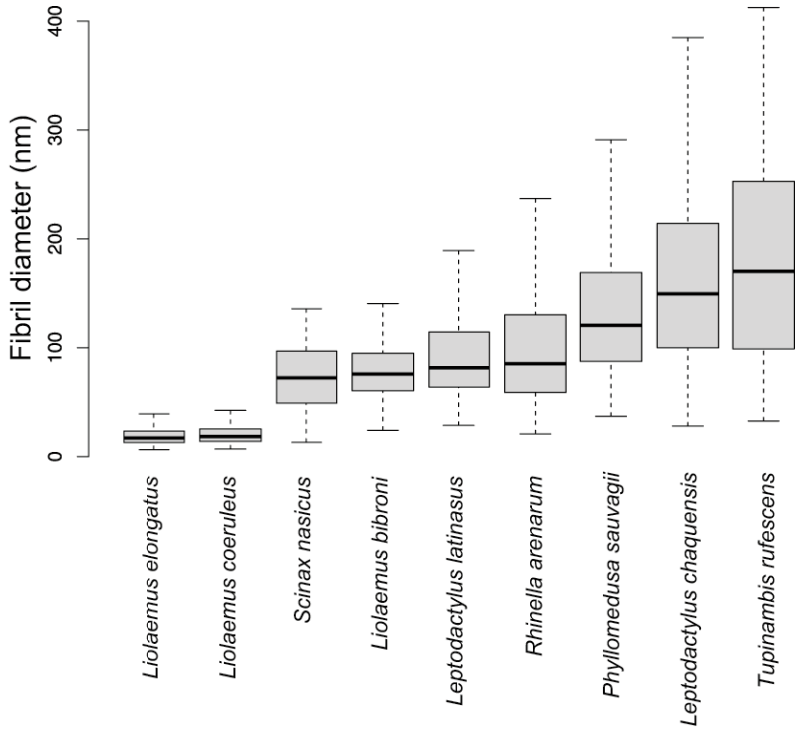

Fig. 2 Size distribution of digital flexor tendon fibrils across some representatives of South American herpetofauna. For each species, data coming from all samples were pooled into a single data set. Species can be segregated into three size categories: one dominated by small fibrils (< 50 nm), another characterized by intermediate fibrils (50-100 nm) and the last one where large fibrils prevail (> 100 nm). Outliers have been removed and whiskers extend to the most extreme data point which is no more than 1.5 times the interquartile range from the box.

Table 1 Percolation characteristics of tendon cross sections.

Species	Number of sampling images analyzed	Average percolation threshold		Percentage of images that resulted in a high percolation threshold (P< 0.05)	Median of the fibril size at the observed percolation threshold (nm)
		Trageted activation	Random activation		
Tupinambis rufescens	1	0.72	0.53	100%	241
Leptodactylus chaquensis	11	0.62	0.51	82%	187
Phyllomedusa sauvagii	7	0.65	0.48	100%	153
Rhinella arenarum	3	0.63	0.49	100%	92
Leptodactylus latinasus	5	0.59	0.49	80%	89
Scinax nasicus	1	0.65	0.48	100%	88
Liolaemus bibroni	1	0.59	0.47	100%	83
Liolaemus coeruleus	1	0.64	0.52	100%	36
Liolaemus elongatus	1	0.70	0.49	100%	23

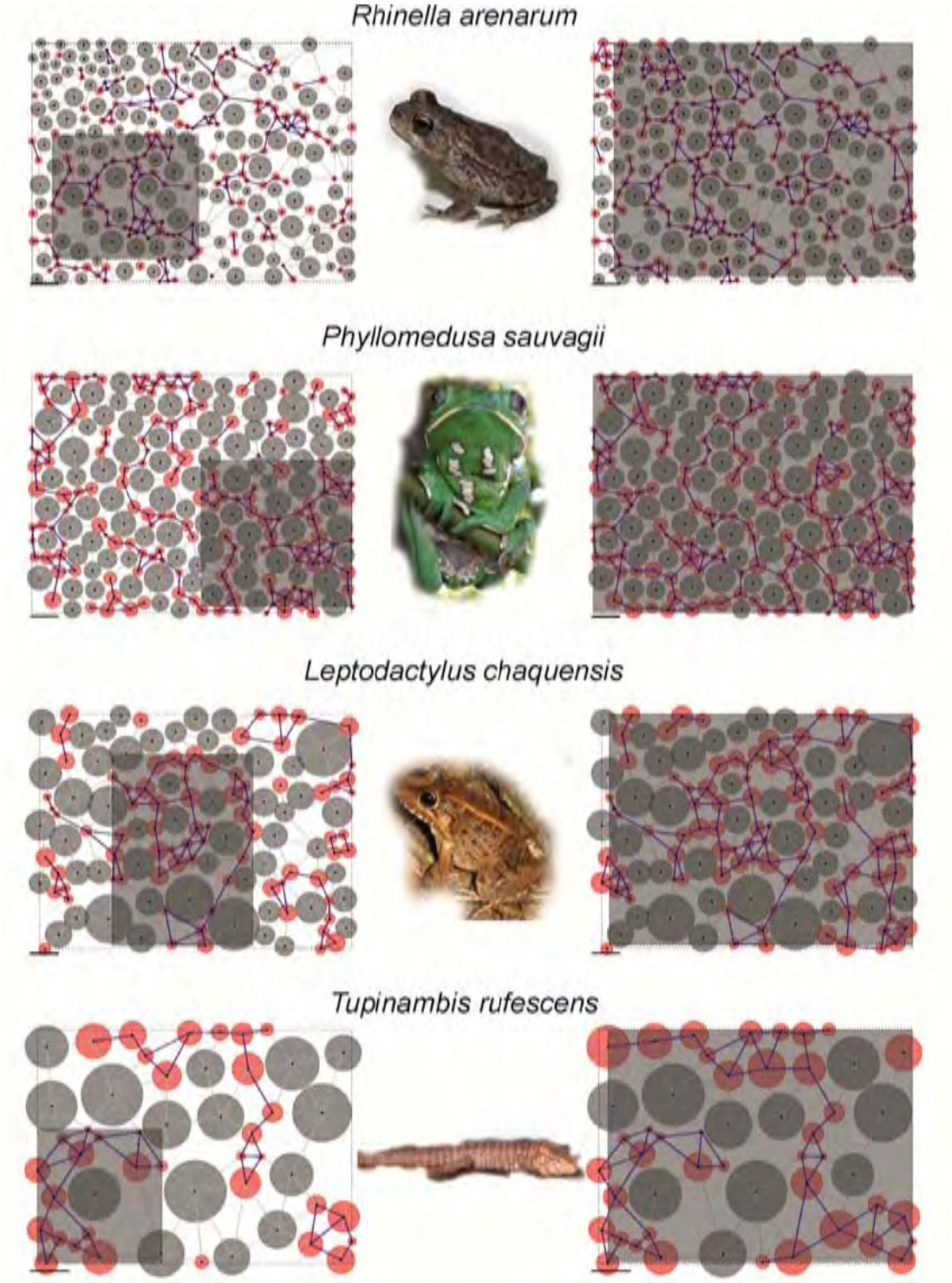

Fig. 3 Fibril proximity networks at two contrasting stages of node activation. Each fibril is proportionally represented to its cross section area. The underlying Gabriel graph (overall inferred network) is also shown and its nodes are located at the mass center of each fibril. Node activation proceeds orderly progressing from the smallest node to the largest one. Images at the left column represent snapshots of networks captured from activation instances close to the formation of the respective percolating clusters. Images at the right column illustrate scenes of fibril recruitment once the percolation threshold had been recently surpassed. As nodes are activated they shift their filling color from grey to red. There exists a blue link between a pair of adjacent nodes if both of them are activated; otherwise they are connected through a grey link. In each scene, dotted bounding boxes for both the study area and the largest component of activated nodes are displayed. Note that the area spanned by the bounding box of the putative percolating cluster (right column) closely matches the entire study area despite some nodes are still inactivated. Scale bars: 250 nm.

In the bulk of data of random simulation, the observed value of percolation thresholds was higher than

random expectancy ($P< 0.05$) (Table 1).Random simulations revealed that there is a geometrical pattern linked to the size of the fibrils in most of the samples, because the percolation occurs at earlier stages of the progressive recruitment when the attribute size for the fibrils is randomly decoupled from the true location of them (Fig. 4). With a slight abuse of words, the high values of percolation thresholds detected imply a geometrical pattern constrained by size.

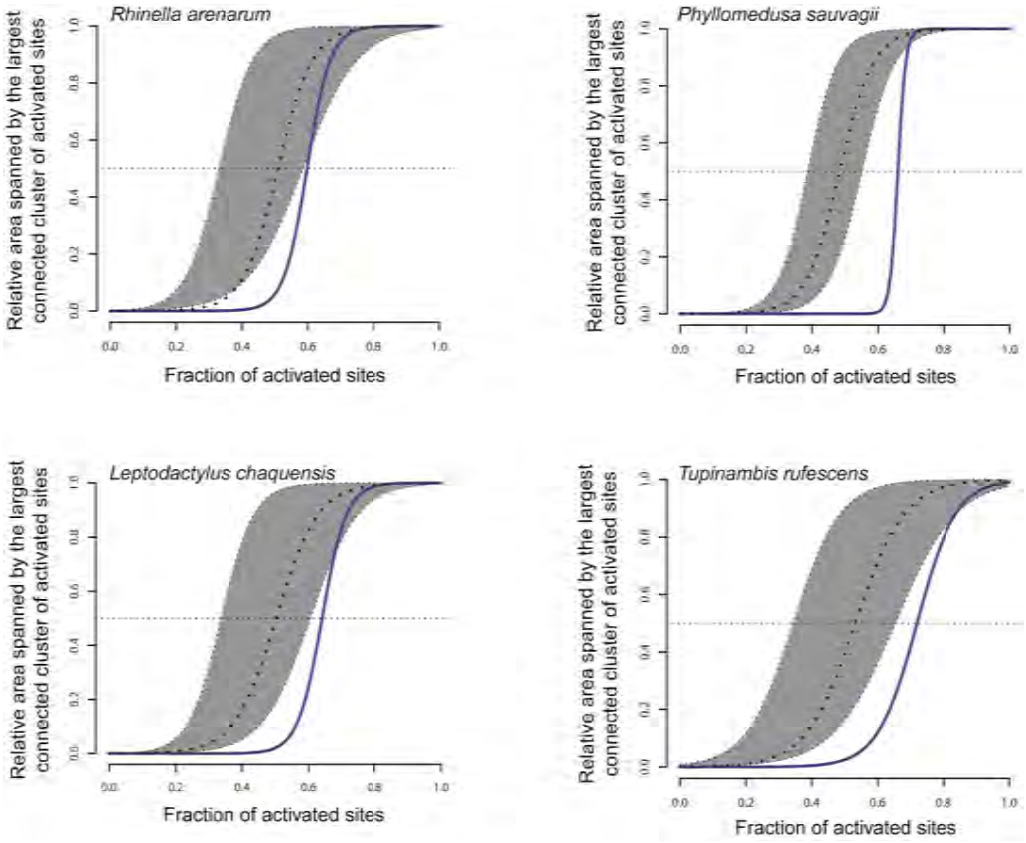

Fig. 4 Percolation curves. The percolation threshold is estimated as the inflection point of the adjusted S-shaped curve that relates the fraction of activated fibrils against the relative rectangular area occupied by the largest component of them. The dotted horizontal line passes through the inflection points of fitting curves. For the scenario of progressive size-dependent recruitment of fibrils (blue curve), the respective percolation threshold falls always beyond the one-sided 95% confidence interval. Confidence intervals were created after considering the curve parameters associated to 100 scenarios of random recruitment of fibrils.

3.2 Balanced interspersion of polymorphic fibrils

We have been able to reproduce conditions of delayed percolation through a non-random layout of heteromorphic units (elements of different sizes) on a square lattice. The pattern under consideration is called by us as Balanced Interspersion of Polymorphic Units (BIPU). BIPU consists of a regular alternated occurrence of larger and smaller fibrils throughout the physical dimensions of the system. Once the pool of fibrils has been partitioned into two sets of contrasting sizes (large and small), we allocate them following a chess board pattern (Fig. 5). Sequential activation of sites in this pre-ordered template may achieve a percolation threshold similar to the observed ones in the analysis of cross-section images of tendon ultrastructure, i.e. $q \sim 0.64$ (Table 2).

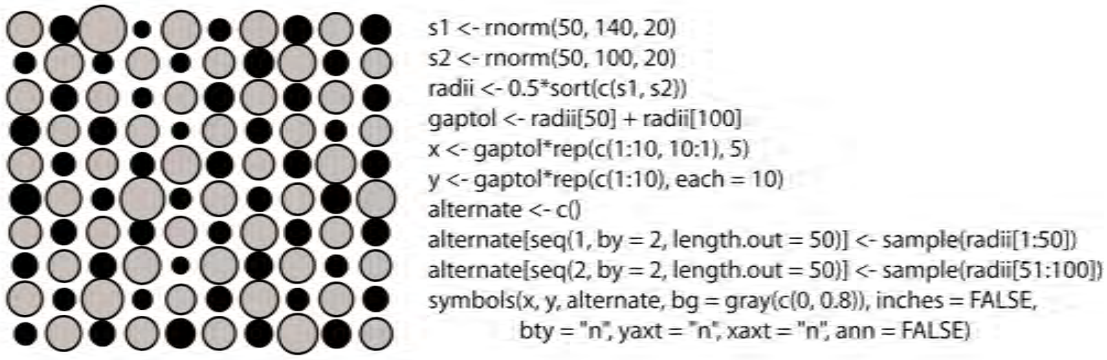

Fig. 5 Model of balanced interspersion of polymorphic fibrils. One hundred fibrils have been sampled from two different distributions of cross section diameter in nanometers. Fifty elements were drawn from a normal variable S_1 ~ (140, 20) whereas the other fifty elements were sampled from S_2 ~ (100, 20). Subsequently, the totality of elements is arranged across a 10 X 10 square lattice where the larger elements (in any order) alternate with the smaller ones (in any order) in a chess board pattern. For an easy backtracking of ideas, the generating R script is displayed next to the respective layout.

Table 2 Statistical synthesis (mean plus minus standard deviation) of percolation experiments performed on several hypothetical square lattices in which putative fibrils of various sizes were allocated following the pattern of balanced interspersion (chess board layout where larger fibrils alternate side-to-side with smaller fibrils). For each lattice configuration, 100 replications were run.

Size of the square lattice	Targeted activation	Random activation
10 X 10	0.65 (± 0.03)	0.52 (± 0.05)
10 X 11	0.66 (± 0.03)	0.52 (± 0.05)
10 X 12	0.65 (± 0.03)	0.51 (± 0.05)
11 X 11	0.66 (± 0.03)	0.51 (± 0.05)
11 X 12	0.66 (± 0.03)	0.52 (± 0.05)
11 X 13	0.67 (± 0.03)	0.52 (± 0.05)
12 X 12	0.66 (± 0.03)	0.52 (± 0.06)
12 X 13	0.65 (± 0.03)	0.52 (± 0.05)
12 X 14	0.66 (± 0.03)	0.53 (± 0.05)
13 X 13	0.66 (± 0.03)	0.52 (± 0.05)
13 X 14	0.66 (± 0.03)	0.52 (± 0.05)
13 X 15	0.66 (± 0.03)	0.52 (± 0.04)
14 X 14	0.66 (± 0.03)	0.53 (± 0.04)
14 X 15	0.67 (± 0.03)	0.52 (± 0.05)
14 X 16	0.66 (± 0.02)	0.52 (± 0.05)
15 X 15	0.66 (± 0.03)	0.53 (± 0.05)
15 X 16	0.66 (± 0.02)	0.52 (± 0.04)
15 X 17	0.66 (± 0.02)	0.53 (± 0.04)
16 X 16	0.66 (± 0.03)	0.53 (± 0.05)
16 X 17	0.66 (± 0.03)	0.53 (± 0.04)
16 X 18	0.66 (± 0.02)	0.53 (± 0.04)
17 X 17	0.67 (± 0.03)	0.53 (± 0.04)
17 X 18	0.66 (± 0.02)	0.53 (± 0.04)

17 X 19	0.66 (± 0.02)	0.53 (± 0.03)
18 X 18	0.66 (± 0.02)	0.53 (± 0.04)
18 X 19	0.67 (± 0.02)	0.53 (± 0.04)
18 X 20	0.67 (± 0.02)	0.54 (± 0.04)

3.3 Stress-strain relationship and inflection point

Typical stress-strain curves for anurans and squamatans digital flexor tendons are shown in Fig.6. Ultimate tensile stress (UTS) for each species and summary statistics about the stress and strain found at the inflection point are showed in Table 3.

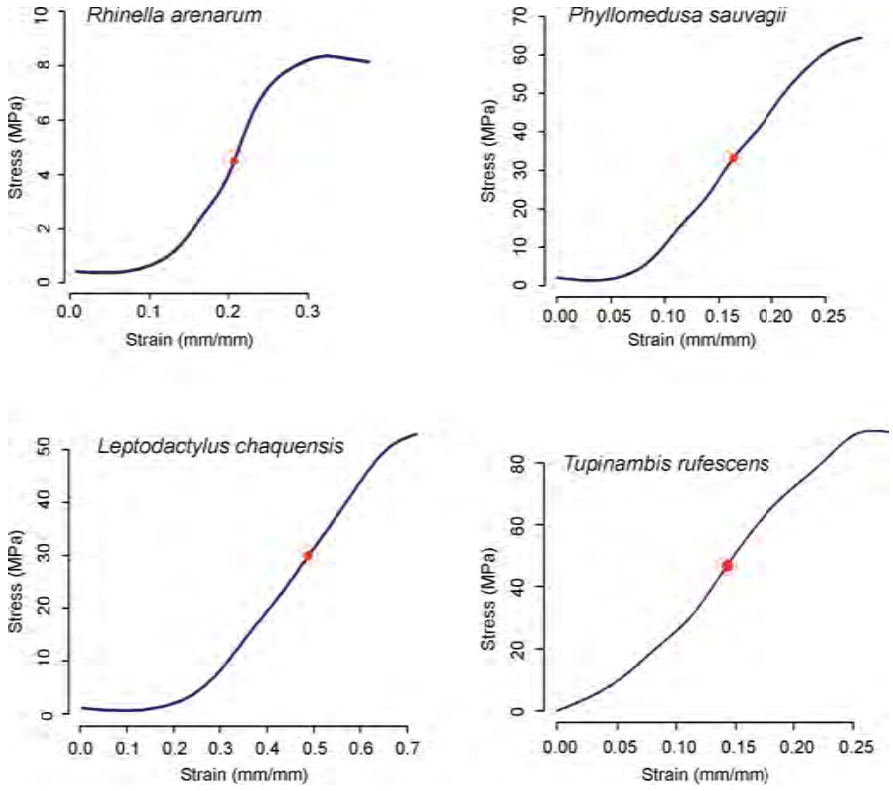

Fig. 6 Stress-strain curves. Direct readings from the Instron® device were adjusted through piecewise-cubic splines. Inflection points marked as red dots.

Table 3 Basic measurements of stress-strain relationship. Reported values are the medians of the respective samples. Scores of critical strain and stress are those recorded at the inflection point of the polynomial cubic fit of the empirical data. Maximum stiffness corresponds to the slope of the tangent at such inflection point. UTS= ultimate tensile strength.

Species	Strain at UTS (mm/mm)	UTS (MPa)	Criticalstrain (mm/mm)	Critical stress (MPa)	Maximumstiffness (MPa)
Rhinella arenarum(n = 6)	0.36	11.22	0.25	6.64	81.27
Phyllomedusa sauvagii (n = 5)	0.23	65.50	0.16	50.14	569.65
Leptodactylus chaquensis (n = 6)	0.62	51.49	0.45	29.82	176.56
Tupinambis rufescens(n = 5)	0.27	47.52	0.15	21.89	488.13

4 Discussion

The survival of living organisms is dependent on the functional integrity of all their organs and organ systems. The tendon is a biomechanical system of force transference from muscles to bones in which its functional integrity translates into a controlled movement of joints. Without loss of generality, the functional integrity of any system relies on the ability of their components to propagate information and offer an adaptive response to external influences. It is hard to conceive such a property in a system of poorly connected components or, equivalently stated, in a system with a relaxed network structure underpinning it. In this paper, we have assumed a network organization for the fibrils of the tendon and consequently explored the patterns of connections between them under the approach of network percolation. At least to our knowledge, percolation theory is the most adequate conceptual framework to answer inquiries about the functional integrity of the tendon, because it deals explicitly with the subject of information propagation throughout the physical dimensions where the system resides.

While Svensson et al. (2013) have recently pointed out that fibrils are not evenly loaded within the tendon butare sequentially recruited throughout the initial stress-strain region, the analysis of our data revealed moreover a size-dependent effect for that sequential recruitment of fibrils. The percolation thresholds are consistently biased towards the upper tail of the statistical distribution of the size of fibrils. It is then comprehensible that the following taxa: *Leptodactylus chaquensis*, *Phyllomedusa sauvagii*, and *Tupinambis rufescens*, exhibit great values for the percolation threshold size. All they surpass easily the 100 nm of diameter in the cross section of fibrils. Ultimately, this means that taxa with great fibrils do not achieve percolation by activation of their small fibrils alone, larger fibrils are also necessary to be activated. A marginal essay performed by us using images about tendon ultrastructure available from literature (horse: Parry, 1988; mouse: Ameye et al., 2002; rabbit: Gill et al., 2004) showed the same pattern. In mammals it also seems to be necessary the activation of fibrils around the 65th percentile to achieve percolation. When compared with the random activation of fibrils, the observed values for percolation thresholds also resulted significantly higher than random expectations.

The delay detected for the occurrence of percolation during the recruitment process indicates that collagen fibrils are spatially arranged according to a geometrical non-random model, in which the location and size attribute are both important. We propose the model BIPU of fibril arrangement characterized by the even interspersion of fibrils of different size category throughout the ECM. This pattern would account for a uniform fibrillar density, that makes restricted regions to be very similar with regards of the overall tendon, and also would explain the delayed percolation threshold observed along our experiments of targeted sites activation. In fact, the balanced interspersion of polymorphic unit simply that larger fibrils makes a shadow effect on nearby smaller fibrils decreasing thus the chance of direct connections between the latter ones. Additionally, the balanced interspersion would also imply that heterogeneous fibrilsare close each other facilitating the access to information managed by the different fibrils. An open question is if the delay for percolation represents a way to optimize the physiological range of tendons.

Traditionally, a typical stress-strain curve for a tendon has been characterized by three regions: the toe, linear and non-linear regions (Wang, 2006). On the contrary, we interpret the resulting stress-strain curve as composed by two phases: the convex and concave regions, being the point of inflection the transition between them. Functionally, they would reflect two quite different behaviors: in the first region, stiffness increases by a targeted activations of fibrils depending upon their sizes, whereas in the second region the tendon begins to yield and fracture. This change in the approach to analyze the stress-strain curve abruptly breaks with the conventional perspective of considering an intermediate linear region in which the respective slope reflect some biomechanical property intrinsically linked to the structure of tendons. In other words, we think that the

task of calculating the Young's modulus as a unique and distinctive measure seems to be a sum-zero exercise in analyzing functional tendon properties. Consequently, we propose to rely on the point of inflection to calculate several metrics that account for the mechanical properties of tendons such as critical stress, critical strain (physiological range), and critical stiffness. We propose an isomorphic linkage between stress-strain and percolation curves, and we hypothesize that the inflection points of both curves reflect a phase transition associated to the same underlying process. This process is probably the propagation of fibril disfunction throughout the extracellular ground of connective tissue. When failure percolates the overall system begins to elongate elastically, so the percolation threshold could indicate the upper bound for the physiological range of the tendon.

In our approach, the physical properties of a tendon depend on the pattern of connections behind the geometrical network of fibrils where location and difference in size play a key role. It is interesting to note that a polimodal distribution of fibril sizes characterize those connective tissues able to resist tensional forces such as tendons. On the contrary, those connective tissues that are commonly under no tensile force show a typically unimodal distribution of fibril size (e.g. buccal gingival mucosa collagen: Ottani et al., 1998; skin collagen: Danielson et al., 1997; Silver et al., 2001; corneal stroma lamella: Parry et al., 1978). Likewise, those tendons that are not yet functional, such as embryonic tendons exhibit also anunimodal distribution of collagen fibril size (Fleischmajer et al., 1988; Parry et al., 1978; Zhang et al., 2005). Unimodal distribution of collagen fibril size is also present in regenerated tendons (Gill et al., 2004). We suggest that for acting efficiently, the polymorphism must be accompanied of another geometrical feature of spatial organization. This spatial organization seems to be subsumed into a pattern of balanced interspersion of different fibrils throughout the ECM. An immediate application of our proposal concerns with the design of strategies for tissue engineering provided of biomimetic-synthetic nanofibrous composites.

5 Concluding Remarks

The polymorphic nature of collagen fibrils in addition to the presence of molecular cross-links between them lead us to think in an heterogeneous network of fibrils that influences the mechanical behavior of tendon as a whole. The main contribution of our work is to combine geometrical and network considerations into a single framework by using the percolation approach. This analysis allows a holistic study of the structural properties of a tendon based on their architectural design. The geometrical pattern we have suggested (non-random packing constrained by size) is amenable with the idea of a progressive and sequential recruitment of fibrils dependent on their size. This pattern offers a delay to percolation, which could act a mechanism for expanding the physiological range. As a surplus of our work, we also address the circumstance of being percolation curves mirrored by the empirical curves of stress-strain obtained from the same studied tendons. By virtue of this isomorphism, we hypothesize that the inflection points of both curves are different quantitative manifestations of a common transitional process during mechanical load transference.

Appendix Specimens examined

L: personal collection of María Laura Ponssa; FBC: personal collection of Felix B. Cruz; FML: Fundación Miguel Lillo; GS: personal collection of Gustavo Scrocchi; ST: personal collection of Sebastián Torres. An asterisk is appended to the access number if the respective specimen was used for studying cross sectional tendon images, otherwise specimens were used for stress-strain analysis.

Leptodactylus chaquensis: *L103, L766, L850*, L344, L950, L950-951*, L964*, L971*, ST103; Leptodactylus latinasus*: *L937a*, L939-942*, L944-945*;*

Phyllomedusa sauvagii: *L849*, L936*, L938*, L946-947, L947(1), L946-948*, L971;*

Rhinella arenarum: *L51, L851*, L909, L935, L935*, L937b*, L961, L965;*
Scinax nasicus: *L949*;*
Liolaemus bibroni: FBC 1265*;
Liolaemus coeruleus: FBC 1265*;
Liolaemus elongatus: GS3227;
Tupinambis rufescens: FML 07256*, FML7554.

Acknowledgements

This work was supported by the ANPCyT and CONICET through the following research grants: PICT 2012-1067, PICT 2012-1910, PIP 112-200801-00225, and BID-PICT 606. All authors are grateful to CONICET for supporting our work via its program of post-graduate fellowships and research grants. We thank Gabriela Pacios (Facultad de Odontología, Universidad Nacional de Tucumán)for assistance with Instron, and NicolásNieva (Facultad de Ciencias Exactas, Universidad Nacional de Tucumán) for comments that greatly improved the structure of the manuscript.

References

Ameye L, Aria D, Jepsen K, et al. 2002. Abnormal collagen fibrils in tendons of biglycan/fibromodulin-deficient mice lead to gait impairment, ectopic ossification, and osteoarthritis. FASEB J, 16: 673-680

Battaglia TC, Clark RT, Chhabra A, et al. 2003. Ultrastructural determinants of murine achilles tendon strength during healing. Connective Tissue Research, 44: 218-224

Berthod F, Germain L, Li H, et al. 2001. Collagen fibril network and elastic system remodeling in a reconstructed skin transplanted on nude mice. Matrix Biology, 20: 463-473

Berkowitz B, Ewing RP. 1998. Percolation theory and network modeling applications in soil physics. SurvGeophys, 19: 23-72

Callaway DS, Newman MEJ, Strogatz SH, Watts DJ. 2000. Network robustness and fragility: percolation on random graphs. Physical Review Letters, 85: 5468-5471

Chandran PL, Barocas VH. 2006. Affine versus non-affine fibril kinematics in collagen networks: theoretical studies of network behavior. Journal of Biomechanical Engineering, 128: 259-270

Christopoulos DT. 2012. Developing methods for identifying the inflection point of aconvex/ concave curve. arXiv:1206.5478v1 [math.NA]

Cuestas E, Vilaró M, Serra P. 2011.Predictibilidad de la propagación espacial y temporal de la epidemia de influeza A-H1N1 en Argentina por el método de percolación. Revista Argentina de Microbiología, 43: 186-190

Danielson KG, Baribault H, Holmes DF, et al. 1997. Targeted disruption of decorin leads to abnormal collagen fibril morphology and skin fragility. Journal of Cell Biology, 136: 729-743

Ferrarini A. 2013. Exogenous control of biological and ecological systems through evolutionary modeling. Proceedings of the International Academy of Ecology and Environmental Sciences, 3(3): 257-265

Ferrarini A. 2014. True-to-life friction values in connectivity ecology: Introducing reverse flow connectivity. Environmental Skeptics and Critics, 3(1): 17-23

Fleischmajer R, Perlish JS, Timpl R, et al. 1988. Procollagen intermediates during tendon fibrillogenesis. Journal Hist Cyt, 36: 1425-1432

Gabriel KR, Sokal RR. *1969.* A new statistical approach to geographic variation analysis. Systematic Zoology,

18:259-278

Gill SS, Turner MA, Battaglia TC, et al. 2004. Semitendinosus regrowth. Biochemical, ultrastructural, and physiological characterization of the regenerate tendon. American Journal of Sports Medicine, 32: 1173-1181

Grimmett G. 1999. Percolation (2nd edition). Springer-Verlag, New York, USA

Jaromczyk JW, Toussaint GT. 1992. Relative neighborhood graphs and their relatives. Proceedings of the IEEE, 80: 1502-1517

Julkunen P, Livarinen J, Brama PA, et al. 2010. Maturation of collagen fibril network structure in tibial and femoral cartilage of rabbits. Osteoarthritis and Cartilage, 18: 406-415

Långsjö TK, Arita M, Helminen HJ. 2009. Cartilage collagen fibril network in newborn transgenic mice analyzed by electron microscopic stereology. Cells, Tissues and Organs, 190: 209-218

Långsjö TK, Vasara AI, Hyttinen MM, et al. 2010. Quantitative analysis of collagen network structure and fibril dimensions in cartilage repair with autologous chondrocyte transplantation. Cells, Tissues and Organs, 192: 351-360

Mikic B, Schalet BJ, Clark RT, et al. 2001. GDF-5 deficiency in mice alters the ultrastructure, mechanical properties and composition of the Achilles tendon. Journal of Orthopaedic Research, 19: 365-371

Newman MEJ. 2010. Networks: An Introduction. Oxford University Press, Oxford, UK

Newman MEJ, Ziff RM. 2001. A fast Monte Carlo algorithm for site or bond percolation. Physical Review E, 64: 016706

Ottani V, Franchi M, Depasquale V, et al. 1998. Collagen fibril arrangement and size distribution in monkey oral mucosa. Journal of Anatomy, 192: 321-328

Parry DAD. 1988. The molecular and fibrillar structure of collagen and its relationship to the mechanical properties of connective tissue. Biophysical Chemistry, 29: 195-209

Parry DAD, Barnes GRG, Craig AS. 1978. A comparison of the size distribution of collagen fibrils in connective tissues as a function of age and a possible relation between fibril size distribution and mechanical properties. Proceedings of the Royal Society of London B, 203: 305-321

Pawłowska M, Sikorski A. 2013.Monte Carlo study of the percolation in two-dimensional polymer systems. Journal of Molecular Modeling (DOI 10.1007/s00894-013-1892-y).

Purslow PP, Wess TJ, Hukins DWL. 1998. Collagen orientation and molecular spacing during creep and stress-relaxation in soft connective tissues. Journal of Experimental Biology, 201: 235-242

R Core Team. 2012. R: A language and enviroment for statistical computing. R Foundation for statistical computing Vienna, Austria. Available at: http://www.R-project.org/.

Reed CC, Iozzo RV. 2002. The role of decorin in collagen fibrillogenesis and skin homeostasis. Glycoconjugate Journal, 19: 249-255

Rigozzi S, Müller R, Snedeker JG. 2010. Collagen fibril morphology and mechanical properties of the *Achilles tendon* in two inbred mouse strains. Journal of Anatomy, 216: 724-731

Rigozzi S, Stemmer A, Müller R, Snedeker JG. 2011. Mechanical response of individual collagen fibrils in loaded tendon as measured by atomic force microscopy. Journal of Structural Biology, 176: 9-15

Shannon CE. 1948. A mathematical theory of communication. Bell System Technical Journal, 27: 379-423, 623–656.

Shirazi R, Vena P, Sah RL, Klisch SM. 2011. Modeling the collagen fibril network of biological tissues as a nonlinearly elastic material using a continuous volume fraction distribution function. Mathematics and Mechanics of Solids, 16: 707-716

Silver FH, Freeman JW, Devore D. 2001. Viscoelastic properties of human skin and processed dermis. Skin

Research and Technology, 7: 18-23

Svensson RB, Mulder H, Kovanen V, et al. 2013. Fracture mechanics of collagen fibrils: influence of natural cross-links. Biophysical Journal, 104: 2476-2484

Teixeira-Filho PF, Rocha-Barbosa O, Paes V, et al. 2001. Ecomorphological relationships in six lizard species of Restinga da Barra de Marica, Rio deJaneiro, Brazil. Rev Chil Anat, 19: 45-50

Tulli MJ, Abdala V, Cruz FB. 2011. Relationships among morphology, clinging performance and habitat use in Liolaemini lizards. Journal of Evolutionary Biology, 24: 843-855

Wainwright SA, Biggs WD, Currey JD, Gosline JM. 1976. Mechanical Design in Organisms. Edward Arnolds, London, UK

Wang JHC. 2006. Mechanobiology of tendon. Journal of Biomechanics, 39: 1563-1582

Zhang G. 2005. Evaluating the viscoelastic properties of biological tissues in a new way. Journal of Musculoskeletal and Neuronal Interactions, 5: 85-90

Zhang G, Young BB, Ezura Y, et al. 2005. Development of tendon structure and function: regulation of collagen fibrillogenesis. Journal of Musculoskeletal and Neuronal Interactions, 5: 5-21

Zhang WJ. 2012a. Computational Ecology: Graphs, Networks and Agent-based Modeling. World Scientific, Singapore

Zhang WJ. 2012b. Modeling community succession and assembly: A novel method for network evolution. Network Biology, 2(2): 69-78

Zhang WJ. 2012c. Several mathematical methods for identifying crucial nodes in networks. Network Biology, 2(4): 121-126

Zhang WJ. 2013. Network Biology: Theories, Methods and Applications. Nova Science Publishers, New York, USA